Jianguo Deng, Zhiyuan Liang, Shi'en Hui and Qinxin Zhao*

Aging Treatment on the Microstructures and Mechanical Properties of New Groove T92/Super 304H Dissimilar Steel Joints

Abstract: The effect of aging treatment on the microstructures and mechanical properties of new groove T92/Super 304H dissimilar steel joints is studied in this paper. The experimental results show that the heat-affected zone (HAZ) of T92 is mainly composed of coarse-grained and fine-grained martensitic, whereas the microstructure of Super 304H HAZ and weld seam exhibit an austenitic structure. Aging treatment increases the nucleation and growth of second phase particles of the weld joints, especially at T92 side. The weld joints have a low tensile strength (<700 Mpa) and a high tensile strength (>700 Mpa) when the tensile fractures are located at weld seam and T92 base metal, respectively. With increasing aging time, the hardness and tensile strength of the weld joints initially decrease, then increase, and finally stabilize. Moreover, the weld joints have a maximum hardness value at the T92 heat-affected zone. At room temperature condition, the impact absorbed energy reaches the minimum value, which is related to the coarse grain containing equiaxed dendrites in the weld seam.

Keywords: dissimilar steel welding, microstructure, mechanical property, welding groove

PACS® (2010). 62.20.Mk

DOI 10.1515/htmp-2014-0067
Received: April 13, 2014; accepted: July 18, 2014;
published online August 26, 2014

1 Introduction

Dissimilar steel weld joints have been widely used in various fields including thermal power, nuclear power, and petrochemical applications in recent years. In the steam generating system of supercritical and ultra-supercritical power plants, ferritic or martensitic heat-resistant steels are usually used in low-temperature conditions, whereas austenitic heat-resistant steels are used in high-temperature sections [1–2]. Considering their superior performance of the creep rupture strength and high temperature corrosion and steam oxidation resistance, T92 and Super 304H steels are widely used in super critical boilers [3–12]. Therefore, the use of dissimilar steel weld joints is inevitable. However, the performance of T92/Super 304H dissimilar steel joints must be assessed in harsh environments with extreme high temperature.

This study investigates the effect of aging treatment on the microstructures and mechanical properties of the new groove T92/Super 304H dissimilar steel joints. Chen Guohong explored the effect of high-temperature aging (0 h to 3000 h) treatment on the mechanical properties of conventional welding T92/Super 304H dissimilar steel joints. Studies showed that the tensile strength and hardness values initially decreased (0 h to 100 h), then increased (100 h to 1000 h), and eventually stabilized (1000 h to 3000 h), whereas the toughness decreased with increasing aging time. Moreover, the tensile fracture was always located on the T92 base material [13]. Cao Jian studied the relationship between microstructures and mechanical properties of T92/Super 304H welding dissimilar steel joints of V-shaped groove at room temperature [14]. The tensile fractures of the dissimilar steel joints was at the T92 coarse grained heat affected zone rather than weld seams. The lateral orientation and distribution of crystal grains herein contributed to the high tensile strength of the dissimilar steel weld joints, and the minimum hardness value was located at weld seams.

In addition, other researchers investigated the microstructure and mechanical properties of dissimilar steel weld joints [15–23, 26]. Hajiannia studied the microstructure and mechanical properties of AISI 347/A335 dissimilar steel using two welding materials. Results showed that ERNiCr-3 was the best choice for dissimilar steel joints because dissimilar steel joints had a high hardness values and impact absorbing energy and tensile strength [15].

***Corresponding author: Qinxin Zhao:** Key Laboratory of Thermo-Fluid Science and Engineering (Xi'an Jiaotong University), Ministry of Education, Xi'an 710049, China. E-mail: a6234.156@stu.xjtu.edu.cn
Jianguo Deng, Zhiyuan Liang, Shi'en Hui: Key Laboratory of Thermo-Fluid Science and Engineering (Xi'an Jiaotong University), Ministry of Education, Xi'an 710049, China

Table 1: Chemical compositions of experimental materials

	C	Cr	Mo	V	Nb	Ni	Mn	P	S	Si	N	Al	W	B	Cu
T92	0.11	9.0	0.50	0.23	0.06	0.26	0.46	0.015	0.002	0.40	0.05	–	1.64	0.004	–
S304H	0.09	18.33	–	–	0.50	8.90	0.80	0.03	0.001	0.025	0.11	0.009	–	0.001	2.94

Celik studied the microstructures and mechanical properties of St37-2/AISI 304 dissimilar steel joints. The results showed that recrystallized grains were found in dissimilar steel welded joints, and the hardness of the weld seam was lower than that in the heat-affected zone [16]. In the paper "Phase evolution in P92 and E911 weld metals during ageing," [17] uneven and coarse austenite grains were obtained, and the growth of the boundary precipitates leaded to the reduction of the impact absorbed energy.

In this paper, the microstructure, tensile fracture, and impact fracture of dissimilar steel weld joints were characterized using an optical microscope, a scanning electron microscope, and an energy spectrum analyzer. Combined with the mechanical properties of weld joints, the structure and property evolution law of T92/Super 304H dissimilar steel joints used in supercritical power plants were explored.

2 Experimental

T92 and Super 304H steel tubes with sizes of Φ51 mm × 13 mm were selected for the experiment, and their corresponding chemical compositions in accordance with ASME standards, are shown in Table 1. The ERNiCr-3 welding wire with a Φ1 mm specification was selected, and its chemical composition is shown in Table 2.

In this experiment, gas tungsten arc welding was used for the welding of T92 and Super 304H steel tubes, and the welding parameters are shown in Table 3. Dissimilar steel welding uses asymmetric grooves, and the schematic is shown in Fig. 1. The weld gap ranges from 0 mm to 1 mm, and the groove angle is α = 20°. The post-weld heat treatment of T92/Super 304H steel tube after welding was 2 h at 730–760 °C to eliminate the welding residual stress.

Table 2: Chemical composition of the ERNiCr-3 welding wire

C	Mn	Si	P	S	Cr	Ni	Cu	Ti
0.031	2.80	0.04	0.004	0.002	20	69.5	0.02	0.35

Table 3: Dissimilar steel welding parameters

Layer	Current (A)	Voltage (V)	Width (mm)	Wire feed speed (mm/min)	Heater current (A)
1	280	9.3	0	1100	11
2	350	12.4	5.2	7500	36
3	350	13	9.4	7400	38
4	330	12.6	12.6	7100	15

After X-ray nondestructive testing, high temperature aging heat treatment were conducted on the new grooves of T92/Super304H dissimilar steel welded joints, and the aging periods were 0, 2000, 4000, and 8000 h. According to the steam temperature and the metal temperature of modern power plants, 625 °C was more proper as the ageing temperature than that in Ref [13]. Afterward, appropriate metallographic samples containing dissimilar steel weld heat-affected zone and base metal were collected and processed into long strips for tensile and impact tests. SANS and XYB305C were used for tensile and impact tests. A VH-5DC hardness tester was used for the hardness test, and the specific position of this test is shown in Fig. 1.

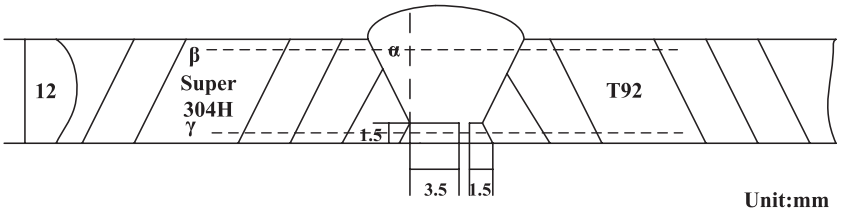

Fig. 1: Schematic diagram of welding process of T92/S304H dissimilar joints and hardness position

Specimens were grinded by SiC papers (up to 2000#), followed by polishing with 0.5 um alumina powders. The welded joints were then etched for 10s to observe the metallurgical structure in each section. Three etching solutions were used as follows: 1) T92: Picric acid 5 mL, ethanol 40 mL; 2) Super 304H: CuSO44g, HCl 20 mL, ethanol 20 mL; 3) weld seam: aqua regia. Finally, an optical microscope (Olympus GX4) and an scanning electron microscope (JED 2200) equipped with an energy dispersive spectroscopy (EDS) were used to observe morphologies of specimens and analyses the precipitated particles. After ultrasonic cleaning with alcohol, the fracture morphologies of the impact and tensile specimens were observed using an scanning electron microscope (JED 2200).

3 Results and discussion

3.1 Microstructure

The heat-affected zone (HAZ) of T92 steel is composed of coarsed and fine-grain HAZ, as shown in Fig. 2. The formation of these grains is correlated with the horizontal distribution of the welding temperature. The welding temperature of fine grain HAZ is close to the austenitizing temperature AC_3, whereas the welding temperature of coarsed grain HAZ is higher than the austenitizing temperature AC_3. The distances of coarsed and fined grain HAZ to the fusion line are approximately 120 and 50 μm, respectively. The fusion line between T92 and weld seam is clear.

Precipitated particles from grains and boundaries are mainly $M_{23}C_6$, as shown Fig. 3 [3–6]. With increasing aging time, the second phase particles grew slowly, but their number gradually increased. The number of precipitated particles in the HAZ is less than that of T92 base metal, causing by the secondary heat tempering of T92 base metal.

The microstructure of Super 304H HAZ is austenite with little crystal twins in Fig. 4. The size of austenite (30 μm) in the HAZ was significantly bigger than that of the base metal (20 μm) due to the high temperature during the welding process. Although the phase transformation temperature was not reached, austenite only grew in the HAZ. The compositions of precipitated particles are shown

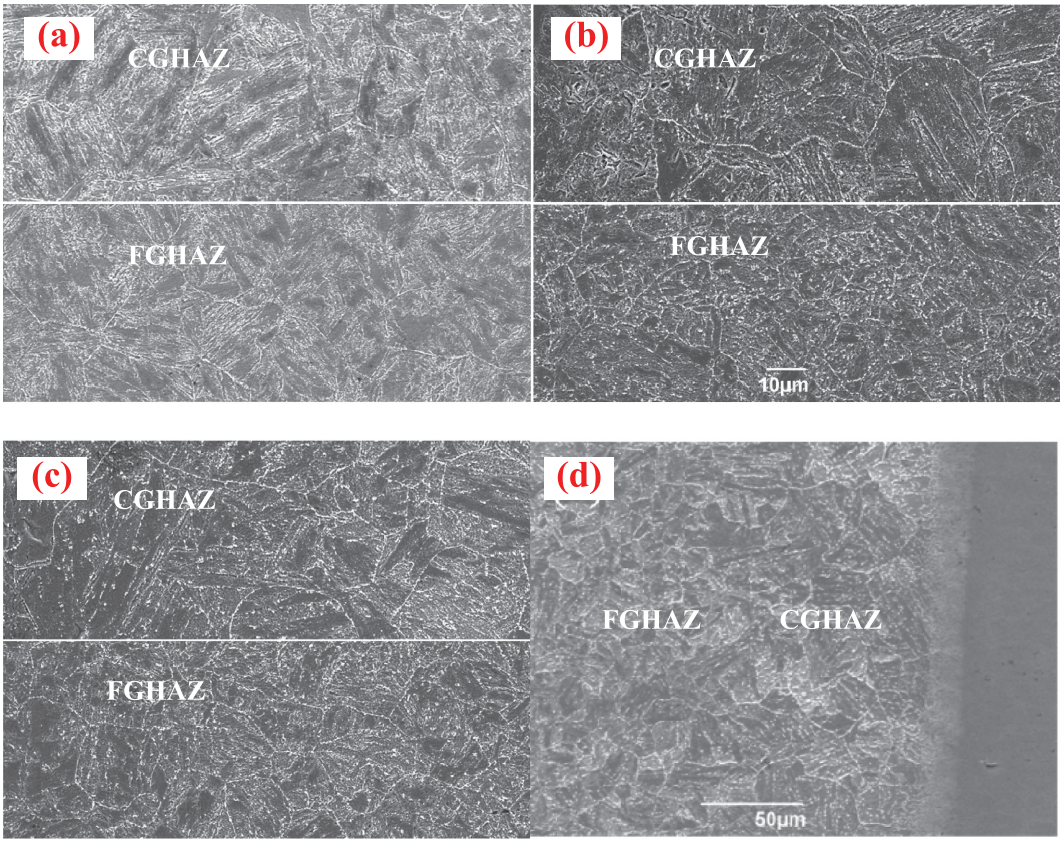

Fig. 2: Microstructures of T92 HAZ: (1) aging 0 kh, (2) aging t 2 kh, (3) aging 4 kh, (4) aging 8 kh

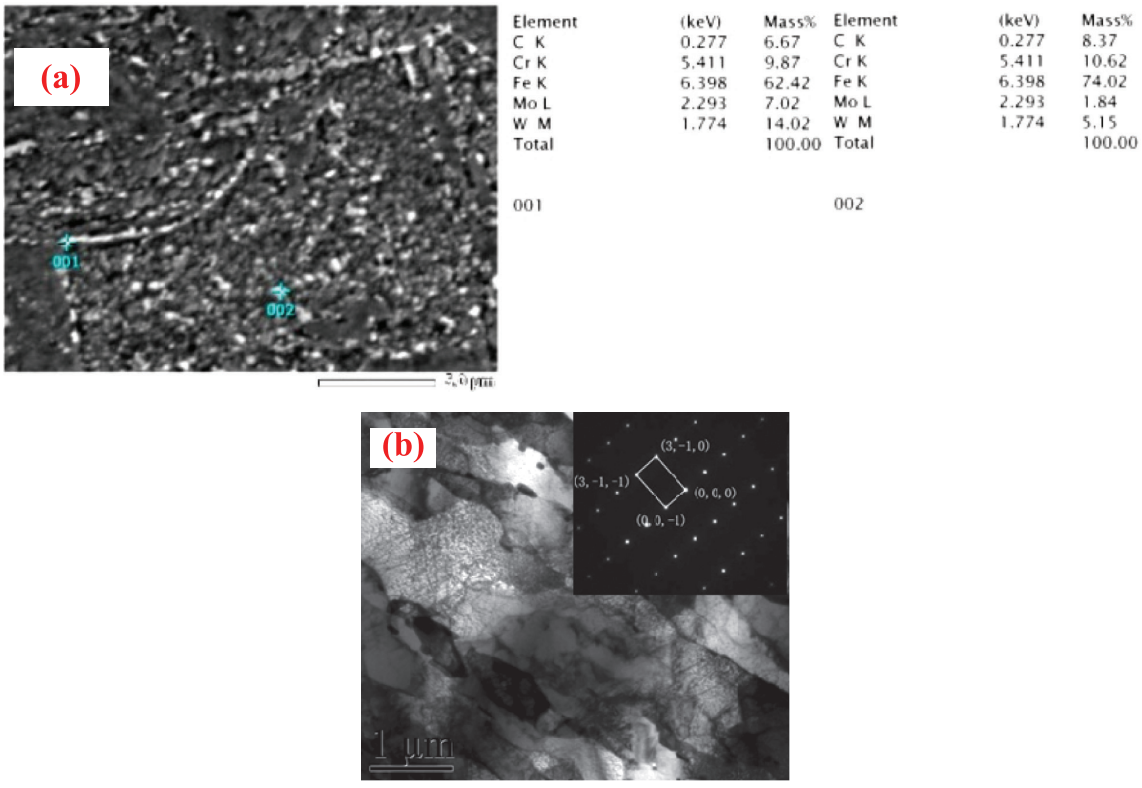

Fig. 3: Precipitate phases in the HAZ of T92. (a) Grain boundary (001) in grain (002), (b) TEM result

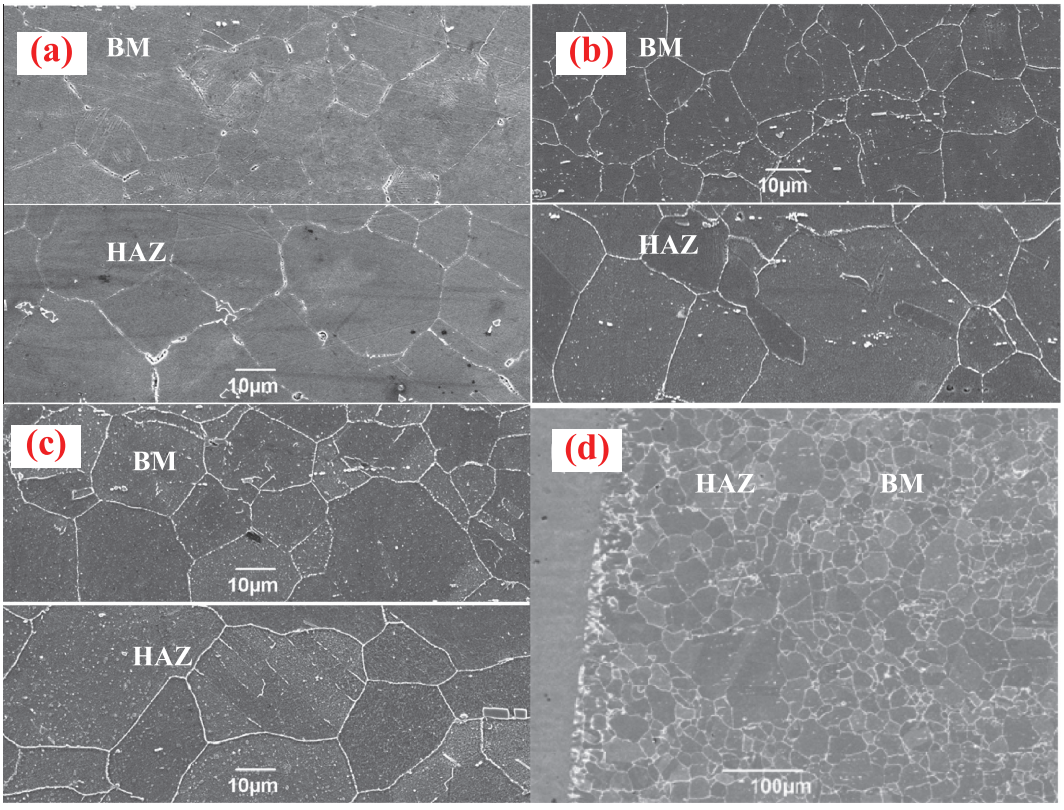

Fig. 4: Microstructures of Super 304H HAZ: (a) aging 0 kh, (b) aging 2 kh, (c) aging 4 kh, (d) aging 8 kh

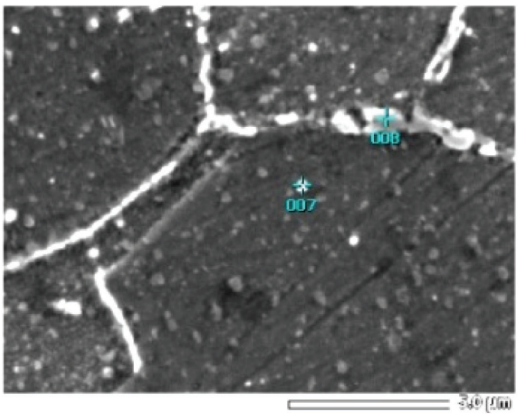

Element	(keV)	Mass%
Cr K	5.411	13.88
Fe K	6.398	40.31
Ni K	7.471	4.93
Nb L	2.166	40.88
Total		100.00

007

Element	(keV)	Mass%
C K	0.277	6.28
Cr K	5.411	28.62
Fe K	6.398	57.60
Ni K	7.471	5.74
Mo L	2.293	1.76
Total		100.00

008

Fig. 5: EDS results of precipitates of the HAZ of Super 304H. Grain boundary (007); In grain (008)

in Fig. 5. Precipitates from grains mainly consist of rich Nb phase, whereas those from grain boundaries mainly consist of $M_{23}C_6$ (M = Fe, Cr) [12]. After aging treatment (2000 h), carbide precipitates appear constantly at the grain boundaries and increase in size, thereby weakening the mechanical properties of the heat-affected zone. Therefore, the rich Nb and the rich Cu phase have an important effect on maintaining the strength of the heat-affected zone. The rich Cu phase can effectively pin dislocations and grain boundaries with less coarsening in the ageing treatment [9–10].

The microstructure of the weld is single austenite with a large grain size, as shown in Fig. 6. When the welding material contains a high amount of nickel element, which is the necessary element for austenite phase, austenite is formed [24]. Meanwhile, the equivalents of Cr and Ni were calculated to be 20.60% and 71.33% based on the Schaeffer equation, respectively. In the common Schaeffer phase

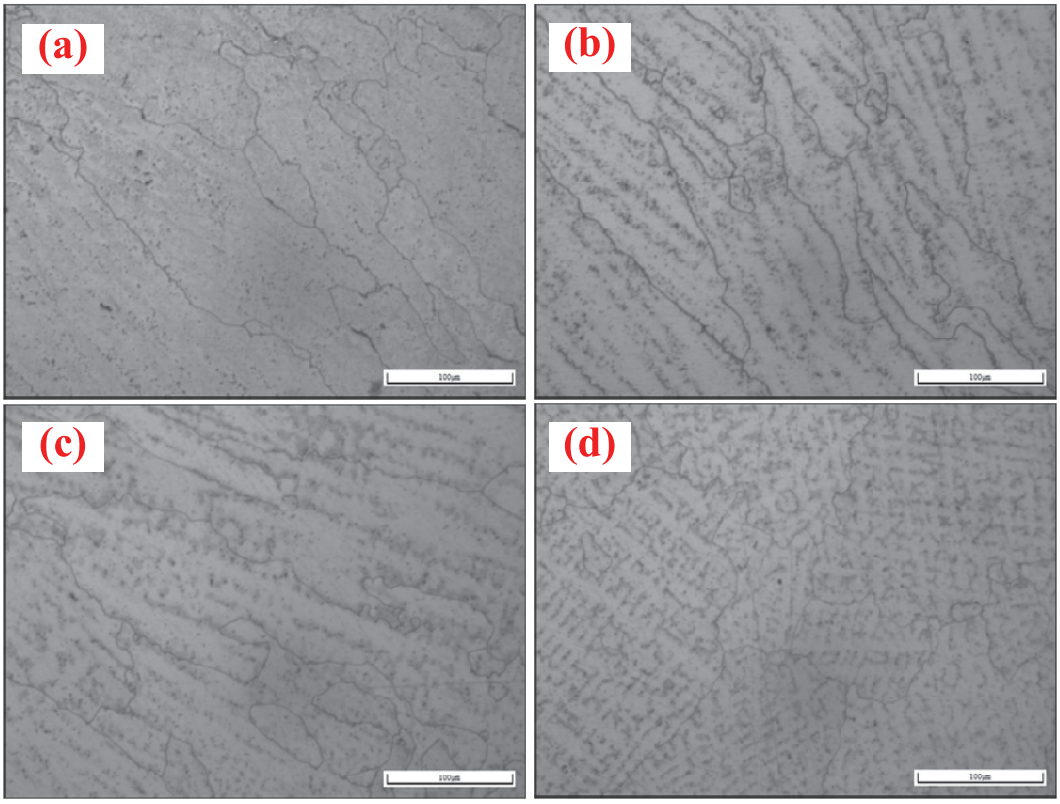

Fig. 6: Microstructure of weld seam: (a) aging 0 kh, (b) aging 2 kh, (c) aging 4 kh, (d) aging 8 kh

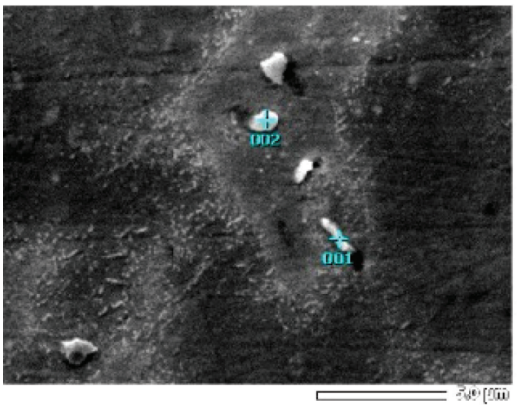

Element	(keV)	Mass%
Ti K	4.508	2.52
Cr K	5.411	10.61
Fe K	6.398	5.72
Ni K	7.471	21.37
Nb L	2.166	59.78
Total		100.00

002

Element	(keV)	Mass%
Ti K	4.508	1.62
Cr K	5.411	20.17
Fe K	6.398	11.54
Ni K	7.471	44.43
Nb L	2.166	22.25
Total		100.00

001

Fig. 7: EDS results of precipitates in weld seams. Strips (001); Spherical (002)

diagram [25], the corresponding location is the austenite phase. However, the slower cooling rate of the metal in the weld pool and a long residence time promote the extremely fast growth of grains because austenite has a low welding thermal expansion coefficient, leading to the poor thermal performance.

A large amount of precipitated particles was found in the grain boundaries and columnar dendrites of the weld seam, as shown in Fig. 7. Precipitated particles shaped strip mainly consist of rich Nb-Ni phase. In Fig. 6(a–c), columnar dendrites and grain boundary migration are observed, whereas in Fig. 6(d), equiaxed dendrites are observed. With increasing aging time, the size of precipitated particles of the weld seam gradually increased.

3.2 Mechanical properties

The tensile strength initially decreased (0 h to 2000 h), then increased (2000 h to 4000 h), and eventually stabilized (4000 h to 8000 h). As shown in Fig. 9, tensile strength values met ASME standards. The fracture morphology changes from ductility to intergranular and subsequently changes into quasi-cleavage fracture. As shown in Fig. 8, the weld joint fracture is located in the weld seam with aging times of 0, 2000, and 4000 h. When the aging time is 8000 h, the welded joints fracture is located in the T92 base metal because the size of austenite grains is basically the same as T92 HAZ. However, the alloying element content of the austenite grain is higher than that of martensite, so the precipitated particles pinned dislocations and grain boundaries. As a result, the strength of T92 HAZ is lower than that of austenite. Moreover, the size of precipitated particles in martensite is significantly greater than those in the T92 HAZ because the T92 base metal experiences two tempering processes. In the tensile test, dislocation effect around the secondary phase particles is counteracted, leading to the decrease of strength. When the tensile strength is less than 700 Mpa, the fracture position is at the weld seam. By contrast, when the tensile strength is higher than 700 Mpa, fracture position is located at T92 base metal.

At room temperature, the toughness of welded joints is higher than ASME standards (49J), as shown in Fig. 9. The impact fracture of Super 304H and T92 were both ductile fracture. In Fig. 10(a) the fracture dimples of Super 304H HAZ were large and deep. The dimple of T92 HAZ was uneven in size. Many small dimples were found in the big dimples in Fig. 10(b). In Fig. 10(c) large and shallow dimples with uneven size were observed, which is directly related to the toughness of the material. Given that T92 HAZ in the welded joints contains coarse and fine-grained, the impact absorbing energy of T92 HAZ is quite different, because it is difficult to control the elongation direction in the rupture process. In Fig. 10(d) the impact fracture had a flat surface on the weld seam, which contains coarse grains with dendritic microstructures. Thus, the toughness of weld seam decreases.

Figure 11 shows the hardness of the weld joint that underwent aging treatment. Overall, the hardness value of T92 HAZ is maximum (280 to 330 HV), whereas that of the weld hardness seam is the minimum (170 to 220 HV). The austenite-martensite transformation occurred in T92 HAZ because the welding temperature is higher than the phase transformation temperature of T92. Thus, a hardened martensitic structure is formed. The hardness of T92 base metal, super 304H base metal, and Super 304H HAZ are almost same. The hardness of the lower weld seam is equal to the hardness of the upper weld seam. Among all the tested aging times, the hardness of the weld joints (2000 h) was minimal.

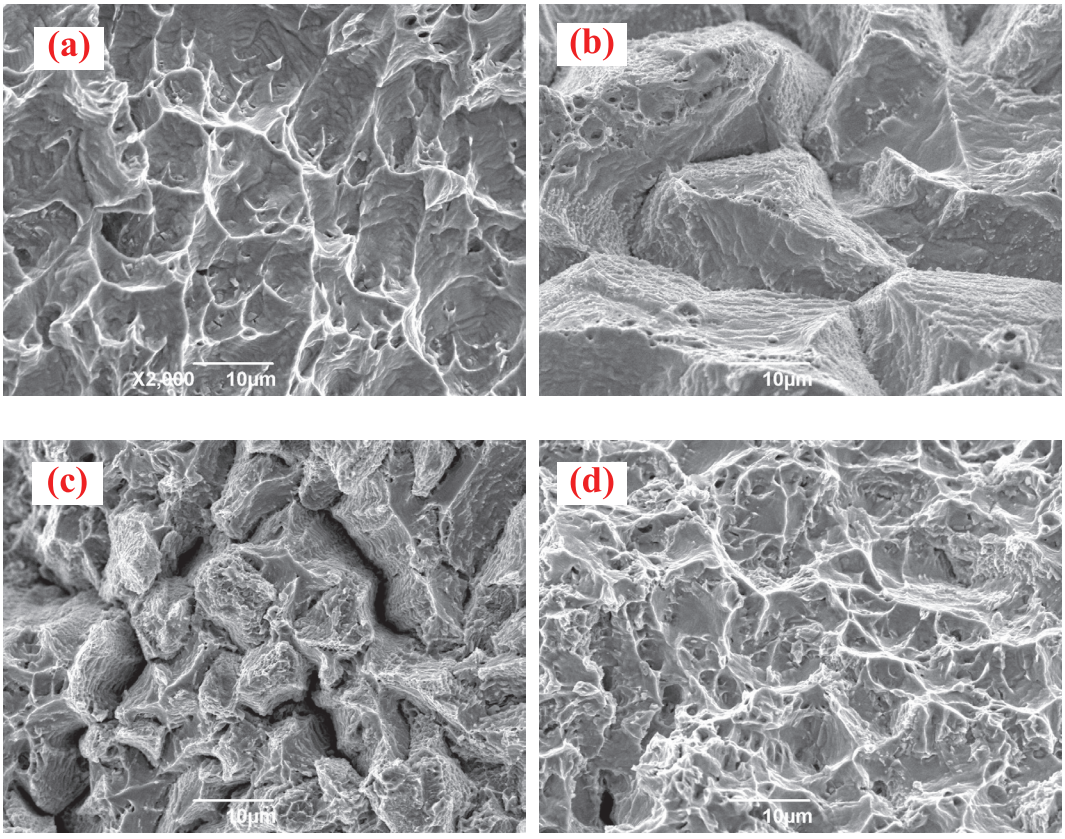

Fig. 8: SEM fractographs of tensile fracture: (a) aging 0 kh, (b) aging 2 kh, (c) aging 4 kh, (d) aging 8 kh

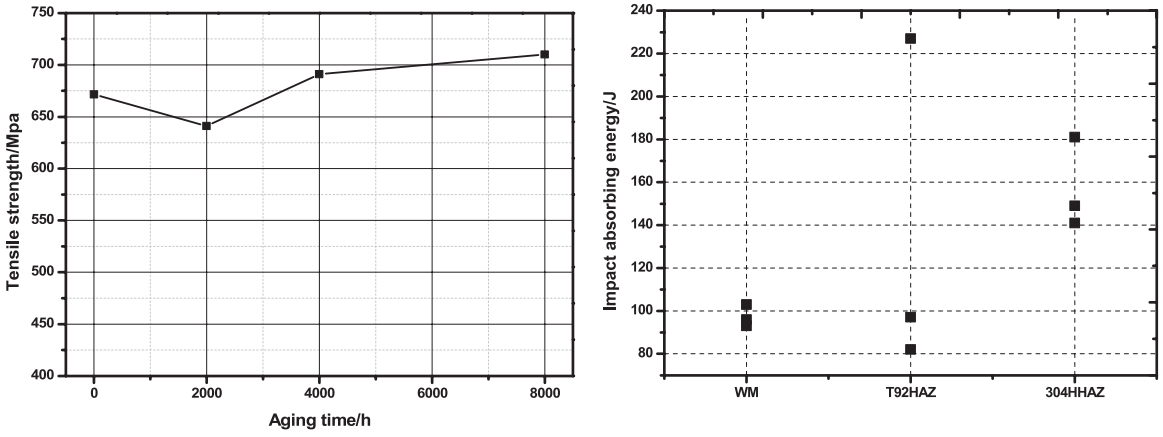

Fig. 9: Tensile test and impact test results T92/S304H dissimilar materials joints

4 Conclusion

1. Super 304H HAZ is composed of coarse austenite. T92 HAZ contains a tempered martensite structures composed of coarse and fine grains. No significant change in the grain size was observed with increasing aging time. The microstructure of the weld seam is composed of the single austenite containing columnar dendrites.
2. The tensile strength, impact toughness at room temperature, and hardness of T92/Super 304H dissimilar steel welded joints at all aging times met the ASME standards. When the tensile strength of the welded joints is less than 700 MPa, the fracture position is

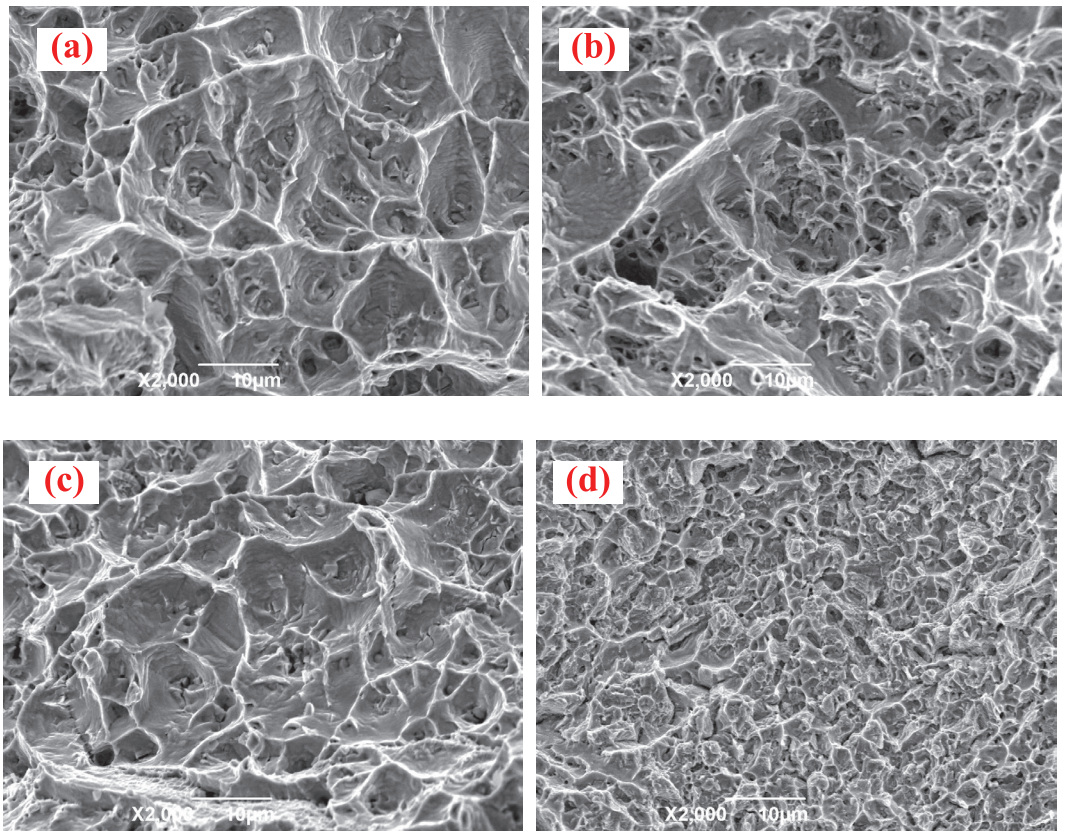

Fig. 10: SEM fractographs of impact fracture: (a) Super 304H, (b–c) T92, (d) weld metal

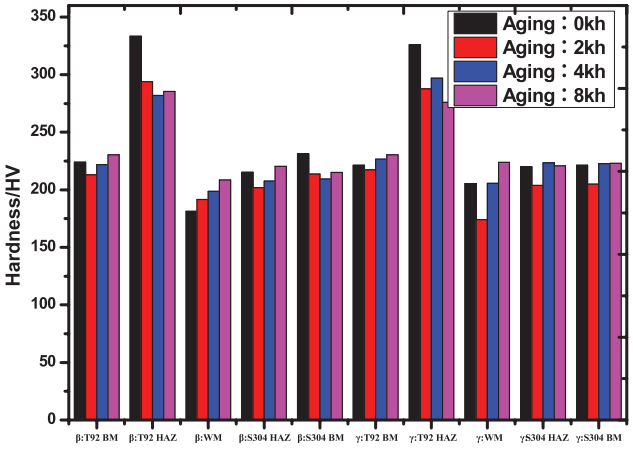

Fig. 11: Hardness test results T92/S304H dissimilar materials joints

located at the weld seam, whereas when the tensile strength is higher than 700 Mpa, the fracture position is located at the T92 base metal.

3. Room temperature impact test results illustrate that the impact toughness of the weld seam is the minimum, which is correlated with coarse and irregular austenite grains of weld seam. The hardness value of the T92 HAZ is significantly higher than in other parts.

Acknowledgments: We would like to thank anonymous reviewers for their helpful comments and suggestions in improving the paper.

Funding: This work was financially supported by National Natural Science Foundation of China (51276133) and the 12th Five-year National Key Technology R&D Program (2011BAK06B04).

References

[1] Celik A, Alsaran A, *Mater. Charact.* 43 (1999) 311–318.
[2] Missori S, Koerber C, *Weld J.* 76 (1997) 125–134.
[3] Ennis P J, Zielinska-Lipiec A, Wachter O, Czyrska-Filemonowicz A, *Acta Mater.* 45 (1997) 4901–4907.
[4] Sklenička V, Kuchařová K, Svoboda M, Kloc L, Bursik J, Kroupa A, *Mater. Charact.* 51 (2003) 35–48.
[5] Sawada K, Kubo K, Abe F, *Mater. Sci. Eng. A.* 319 (2001) 784–787.
[6] Abe F, *Sci. Tech. of Adv. Mat.* 9 (2008) 1–15.
[7] Abe F, Horiuchi T, Taneike M, Sawada K, *Mater. Sci. Eng. A.* 378 (2004) 299–303.
[8] Kimura K, Sawada K, Kushima H, Kubo K, *Int. J. Mater. Res.* 99 (2008) 395–401.
[9] Jiang J, Zhu L, *Mater. Sci. Eng. A.* 539 (2012) 170–176.

[10] Di Schino A, Kenny J M, Mecozzi M G, Barteri M, *J. Mater. Sci.* 35 (2000) 4803–4808.
[11] Iseda A, Okada H, Semba H, Igarashi M, *Energy Mater.* 2 (2007) 199–206.
[12] Sourmail T, *Mater. Sci. Tech.* 17 (2001) 1–14.
[13] Chen G, Zhang Q, Liu J, et al., *Mater. Des.* 44 (2013) 469–475.
[14] Cao J, Gong Y, Zhu K, Yang Z G, Luo X M, Gu F M, *Mater. Des.* 32 (2011) 2763–2770.
[15] Hajiannia I, Shamanian M, Kasiri M., *Mater. Des.* 50 (2013) 566–573.
[16] Celik A, Alsaran A, *Mater. Charact.* 43 (1999) 311–318.
[17] Výrostková A, Homolova V, Pecha J, Svoboda M, *Mater. Sci. Eng. A.* 480 (2008) 289–298.
[18] Dehmolaei R, Shamanian M, Kermanpur A, *Mater. Charact.* 59 (2008) 1447–1454.
[19] Gong Y I, Cao J, Ji L N, Yang C, Yao C, Yang Z G, Hu Z F, *Fatigue Fract. Eng. M.* 34 (2011) 83–96.
[20] Kuo T Y, Lee H T, *Mater. Sci. Eng. A.* 338 (2002) 202–212.
[21] Cao J, Gong Y, Yang Z G, Luo X M, Gu F M, Hu Z F, *Int. J. Pres. Ves. Pip.* 88 (2011) 94–98.
[22] Falat L, Svoboda M, Výrostková A, Petryshynets I, Sopko M, *Mater. Charact.* 73 (2012) 15–23.
[23] Falat L, Výrostková A, Homolová V, Svoboda M, *Eng. Fail. Anal.* 16 (2009) 2114–2120.
[24] Kou S, *Welding Metallurgy*, John Wiley & Sons, New York (1987).
[25] Lippold J C, Kotecki D J, *Welding Metallurgy and Weldability of Stainless Steels*, Wiley-VCH (2005).
[26] Chen G, Song Y, Wang J, et al., *Eng. Fail. Anal.* 26 (2012) 220–229.